JMEPEG (2011) 20:1028–1035
DOI: 10.1007/s11665-010-9715-0

1059-9495/$19.00

Effect of Zincation/Sonication on Electroplated Gold Deposited on Aluminum Substrate

M. Palaniappa, M. Jayalakshmi, and K. Balasubramanian

(Submitted December 29, 2009; in revised form May 15, 2010)

The adhesion strength of gold plated layers on Al substrates has been investigated. Conventional zincation and modified zincation under ultrasonication of aluminum samples are done. Zincation is done by two ways: single zincation and double zincation. Both are repeated under ultrasonic agitation. Ultrasonic agitation during zincating produced dense population of small Zn particles and increased the coverage of Zn intermediate layer. Subsequent nickel strike by electrochemical nickel plating is carried out to form an intermediate nickel layer over the aluminum substrate. As the final step, gold electrochemical plating is done which produced spindle-like gold particles upon the nickel substrate. Gold-plated samples are characterized using E-log *I* polarization, SEM, and adhesion pull-off test. Gold-plated sample pre-treated with double zincation and ultrasonication shows the best result in terms of corrosion potential, surface morphology and pull-off test.

Keywords aluminum substrate, electrochemical gold plating, nickel strike, single and double zincation, ultrasonication

1. Introduction

Electroless plating of aluminum with nickel after zincating the virgin surface is an evolved study to avoid the corrosion of aluminum chips used in flip chip technology. Flip chip technologies are being used in the electronics industry primarily because of their high I/O density capability, short signal paths, and low interconnect parasitic resistance (Ref 1, 2). The relentless miniaturization drive, together with the demand for higher performance and functionality of portable electronic products, such as notebook PCs and hand phones, translates into the use of smaller electronic packages with higher I/O counts operating at higher frequencies. Flip chip packaging technology is currently the most promising approach to satisfy the high-end packaging market. A key contributor to this technology is wafer bumping, whereby interconnection metallic bumps are built on the chip's I/O pads. When the chip is "flipped over" and attached to a matching pattern on a substrate, the bumps provide the interconnection, which is conventionally achieved by wire bonding. Among the various bumping methodologies, the electroless nickel (EN) metallization and bumping process is relatively low cost and straightforward (Ref 3-11). In cases where multi-element lead-free solder is difficult to deposit by electroplating, electroless nickel metallization plus other direct solder application techniques, such as stencil printing, will be a more feasible processing route. Aluminum, with minor doping of other elements, is the dominant material for IC bond pad metallization. Aluminum is catalytic for electroless nickel deposition. However, as aluminum instantaneously oxidizes during rinsing or exposure to air, the oxide films will completely suppress metallization or prevent the formation of intermetallic bonds between the EN and the substrate, resulting in adhesion failure.

Zincating of the aluminum pads is a widely used process step that activates the pads for subsequent EN deposition, which in principle, gives rise to good adhesion between pad and bump. Zincating relies on the electrochemical exchange reaction between zinc complexes in solution and aluminum metal, depositing zinc crystallites at the expense of aluminum dissolution (etching). Several methods have been tried to improve the adhesion between the plated Ni film and the Al pad. The improvement of adhesion by changing of bath chemistry (Ref 12), applying modified deposition techniques of Al substrates (Ref 13), and using a multiple zincate process (Ref 13, 14) were all tried. These methods imply that the zincate morphology control is important to increase the adhesion between the Al pad and the Ni bump. Dense Zn particles give rise to good adhesion between the Al pad and the Ni bump. The multiple zincating process is used widely in industry to improve the adhesion strength between Ni and Al. It provides dense Zn particles, and improves the adhesion of electroless Ni layers. Using a double zincating treatment in which the first zincate treatment is followed by Zn stripping in an acidic solution and then by a second zincating treatment, a smooth and uniform Zn deposition layer is obtained (Ref 12-15). However, the multiple zincating treatment has several problems such as being a complex process and an excess of Al dissolution due to the aforementioned Zn stripping step in a concentrated HNO_3 solution. In electrodeposition, ultrasonic agitation is beneficial to enhance the mass transport of cations to the cathode surface, thus reducing concentration polarization (Ref 16, 17). It was shown that the ultrasonic agitation during zincating produced the dense population of

M. Palaniappa, M. Jayalakshmi, and **K. Balasubramanian**, Non-Ferrous Materials Technology Development Centre, Kanchanbagh Post, Hyderabad 500 058, India. Contact e-mail: mpalaniappa@yahoo.com.

small Zn particles and increased the coverage of a Zn intermediate layer. The uniform Zn layer and the sufficient coverage of Zn particles on Al surface increased the adhesion between Ni and Al surface since electroless Ni deposition is activated on the Zn layer (Ref 18).

In this study, aluminum coupons are (1) single zincated with/without ultra-sonication, (2) double zincated with/without ultra-sonication, (3) given a nickel strike and finally gold plated. The different combinations will help to screen and optimize the experimental conditions to get the best coating. The effect of zincation and ultra-sonication on the morphology and corrosion of gold-plated aluminum coupons are studied.

2. Experimental

2.1 Preparation of Plated Samples

Commercial pure aluminum plates of size 50 × 30 mm were used. The plates were initially cleaned by immersing in dilute (10%) alkaline (NaOH) solution and then in dilute (10%) acidic (HNO_3) solution. After the pretreatment step, the sequence of main processes adopted was as follows: (1) chemical zincating; (2) electrochemical nickel strike; (3) electrochemical gold plating. The complete process sequence is as listed below.

1. mild etching-cleaning with weak alkaline cleaner (10% NaOH);
2. rinsing with deionized (DI) water, room temperature (RT);
3. cleaning in mild acid, RT (10% HNO_3);
4. rinsing with DI water, RT;
5. first zincating; 10 sec, RT;
6. rinsing with DI water, RT;
7. nitric acid dip; 20% HNO_3, 10 s, RT;
8. rinsing with DI water, RT;
9. second zincating; 10 sec, RT;
10. rinsing with DI water, RT;
11. nickel strike, 60 s at 1 A/dm^2, 55-60 °C;
12. rinsing with DI water, RT;
13. gold plating in cyanide bath, 5 min at 2 A/dm^2, 50-55 °C;
14. rinsing with DI water, RT.

Steps 7 to 10 in the process flow sheet were not followed in the case of single zincating process. Zincating was done under ultrasonic agitation (28 kHz frequency) for both single and double zincating. The composition of zincating bath is shown in Table 1. Zincation was done by immersing the pre-cleaned aluminum coupons in the zincating bath for 10 s at room temperature; this chemical process ensures the adhesion of zinc to the aluminum surface. The first zincating step done without and with ultrasonic agitation of aluminum samples were designated as Au-w-o-1 and Au-w-u-1, respectively. The second zincation was done in the same fashion but pretreated with 20% nitric acid and washed. Second zincation was also done without and with ultrasonication and the aluminum samples were designated as Au-w-o-2 and Au-w-u-2, respectively.

Nickel strike was given from a Watt's bath (nickel sulfate 250 g/l, nickel chloride 45 g/l, boric acid 30 g/l) maintained between 55 and 60 °C. Nickel strike was done for a period of 60 s at 1 A/dm^2. Nickel plate was used as anode.

Table 1 Chemical composition of zincating bath

Chemical	Quantity, g/l
ZnO	4
NaOH	120
$NaNO_3$	1
$KNaC_4H_4O_6{\cdot}4H_2O$	50

Table 2 Chemical composition of gold plating bath

Chemical	Quantity
GPC (gold plating cyanide) salt	4.68 g/l (Au 3.2 gpl)
KCN	2.275 g/l (CN^-/Au = $<$0.30)
$K_2Cr_2O_7$	167 g/l
H_2SO_4	8.3 ml/l
HNO_3	16.7 ml/l
KOH	16.7 g/l

The final step was gold plating. The composition of plating bath is given in Table 2. Gold plating was carried out at a current of 2 A/dm^2 for a period of 5 min. Platinum sheet was used as counter electrode. The plating bath was maintained between 50 and 55 °C. Gold plating thickness was estimated by weight difference.

2.2 Instrumentation

Surface morphology of zincated and gold-plated surface was studied using a scanning electron microscope (SEM) TESCAN Vega. All electrochemical experiments were conducted with a PGSTAT 302 Autolab system (Ecochemie, Utrecht, The Netherlands). It was connected to a PC running with Eco-Chemie GPES software. The reference electrode was Ag/AgCl (3 M KCl) and the counter electrode was a platinum wire supplied along with the instrument. The electrolyte solution was 0.1 M H_2SO_4. The electrodes were arranged in a flat cell (Wear and Friction Tech, Chennai) such that 1 cm^2 area of the working electrode (sample) was exposed to the electrolytic medium. Pull-off adhesion test (Defelsko Positest) was done to study the adhesive strength of the Au coating on Al substrate.

3. Results and Discussion

3.1 Analysis of SEM Images

Figure 1a shows the SEM image of Au-w-o-1 sample. Single zincated surface reveals a nonuniform adhesion of zinc particles to the Al substrate. In some spots, the bare Al surface is exposed while there is overlapping of zinc particles in some spots. The Zn nucleation reaction in the zincating is mainly an exchange reaction between Al substrate and Zn ions in the solution. Zn nuclei formed at the beginning of the reaction tend to keep growing into large size particles unless the growth is interrupted. The slow nucleation rate produces the rough deposits which are the mixture of the large and small particles. When the zincation was done with ultra-sonication, the change in deposition is quite noticeable as shown in Fig. 1c. One could see a uniform dispersion of zinc particles as against the one without sonication. These effects will enhance the Zn

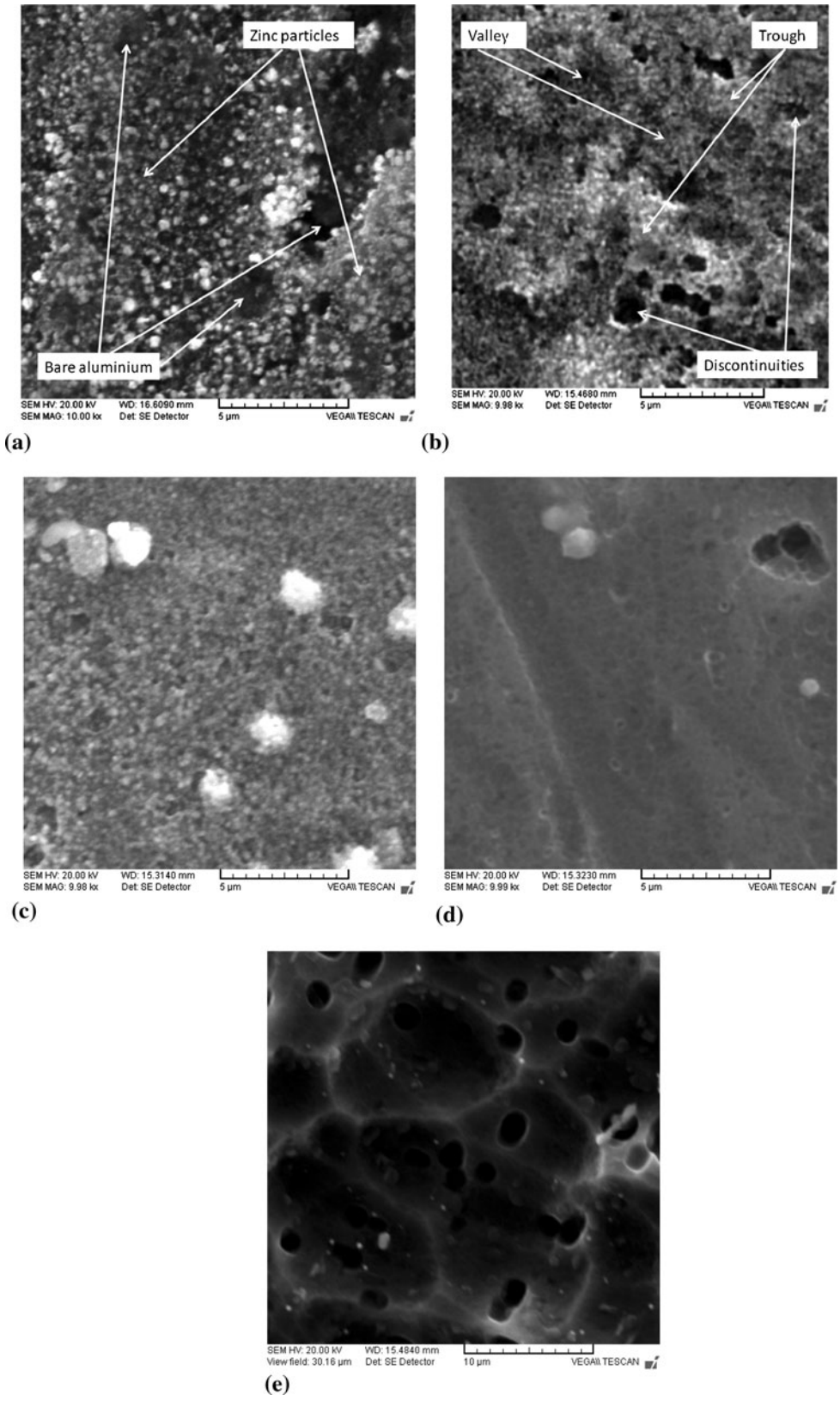

Fig. 1 SEM micrographs of bare and zincated aluminum coupons. (a) Single zincated without ultrasonication, (b) double zincated without ultrasonication, (c) single zincated with ultrasonication, (d) double zincated with ultrasonication, (e) aluminium bare substrate

nucleation on Al surface. The increased nucleation rate and, thus, fine particle distribution by ultrasonic agitation is evident in the specimen which was single zincated for a short time.

Ultrasonication using a bath ultrasonicator is a well-known technique used to disperse carbon nanotubes (Ref 19, 20). Ultrasonication imparts a high energy density in the solution.

Ultrasonication generates alternating low-pressure and high-pressure waves in liquids, leading to the formation and violent collapse of small vacuum bubbles. This phenomenon is termed cavitation and causes high-speed impinging liquid jets and strong hydrodynamic shear-forces. These effects are used for the deagglomeration and milling of micrometer and nanometer-size materials as well as for the disintegration of cells or the mixing of reactants. Cavitation can break the aggregated particles apart, which will improve the dispersion and improve the mechanical property of the deposit. When two particles are separated by a distance of only a few particle diameters, hydrodynamic forces of repulsion and attraction are involved in the ultrasound field (Ref 21). The maximum tensile strength is the balance of the contracting force and repelling force created in the ultrasound field (Ref 22). SEM image in Fig. 1c proves that the time allocated for sonication was sufficient to produce uniform dispersion of zinc particles. Increase in sonication time is also not advisable as it leads to degradation of mechanical properties of the deposit (Ref 23). Thus, there is a trade-off between improving dispersion and damaging the deposit.

Figure 1b shows the SEM image of Au-w-o-2 sample. Double zincation as against single zincation was highly effective in enhancing the deposit of finer zinc particles but the adhesion was not uniform. The deposit has lot of troughs and valleys and large number of discontinuities. When the double zincation was done with ultrasonication, the beneficial effect is highly visible as shown in Fig. 1d (Au-w-u-2). The deposit appears neat with a uniform adhesion and fine dispersion of zinc particle. This result concurs with the earlier report on this topic (Ref 18). The double zincating with ultrasonic agitation produced much smaller and denser Zn particles. The dense particles essentially became a continuous film. Figure 1e shows the SEM micrograph of bare aluminum sample.

Electrochemical Ni deposition is activated on the Zn layer which was provided by the zincate treatment. The adhesion of the Ni layer on the Al substrate depends on the Zn coverage since the Ni layer and Al surface are connected by the Zn intermediate layer. The single zincate treatment in a conventional method formed the Zn particles of various sizes and left many vacant sites on the Al surface, which resulted in the poor Zn coverage on the Al surface. The adhesion of Ni layer on Al substrate was weak; in that case, the gold adhesion shall also be weak.

Gold-plated (~5 μm thick) samples reflect similar characteristics. SEM images of A-w-o-1 sample are shown in Fig. 2a. Higher magnification clearly shows spindle-shaped gold particles deposited in discontinuous fashion with exposed nickel surface. The length of gold spindles is in the range of 400-600 nm. This result confirms the fact previous history of pretreatment have a definite impact on the final deliverable product. Ultrasonication during single zincation improves the dispersion of gold particles as shown in Fig. 2b. Spindle-shaped gold particles lie close neck to neck indicating a finer disposition of particles, in some spots.

Figures 3 (a) and (b) show the SEM images of Au-w-o-2 and Au-w-u-2 samples, respectively. Double zincation ensures dense dispersion of gold particles in both the samples but the effect of ultrasonication on the de-agglomeration of gold spindles is clearly evident in Fig. 3b. Though the particles are deposited neck to neck in both the cases, the dispersion is more coherent and uniform in the sonicated sample. Agglomerations observed in some portions in the nonsonicated sample proclaim the need for sonication for the preparation of uniform plated surface.

3.2 E-log I polarization studies

E-log *I* polarization curve is a potentiodynamic corrosion curve obtained by recording the current output against a range of applied potentials. Corrosion is a process and not just a property of the material. The corrosion potential, therefore, is uniquely characteristic of the physics and chemistry at the solution-surface interface and not just of the alloy itself. This potential is a measure of all the electrochemical processes occurring at the surface and the environmental influence on those processes. Since electrons are exchanged during such a corrosion process, the reactions involved create an electrochemical potential. This potential is called the "corrosion potential or mixed potential". Since the corrosion potential is

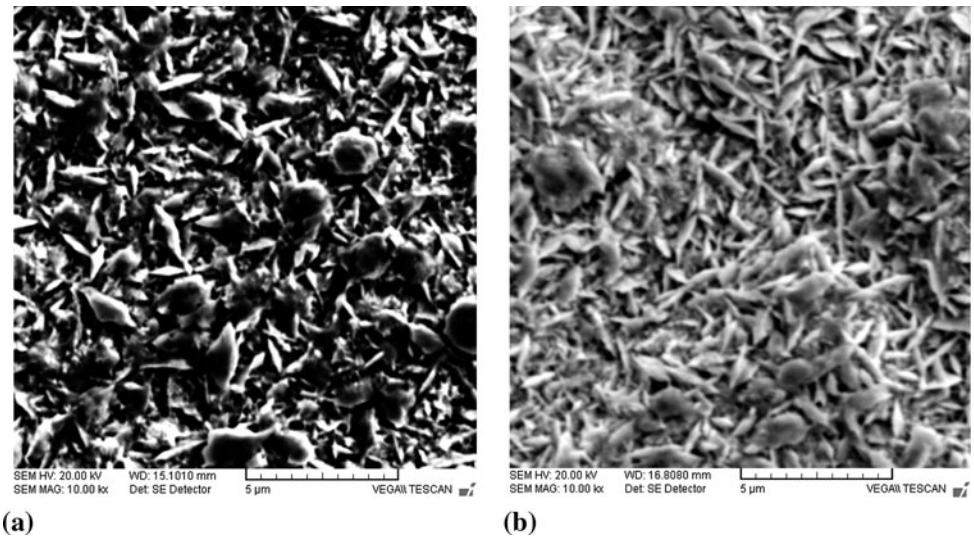

Fig. 2 SEM micrographs of gold plated aluminum coupons. (a) Without ultrasonication—single zincated/gold plated, (b) without ultrasonication—double zincated/gold plated

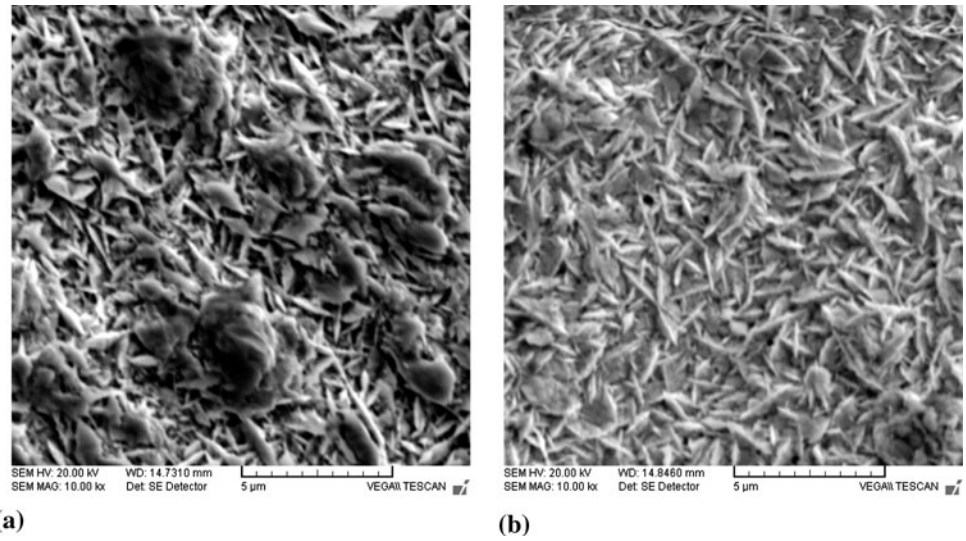

Fig. 3 SEM micrographs of gold-plated aluminum coupons (with ultrasonication). (a) Ultrasonication—single zincated/gold plated, (b) ultrasonication—double zincated/gold plated

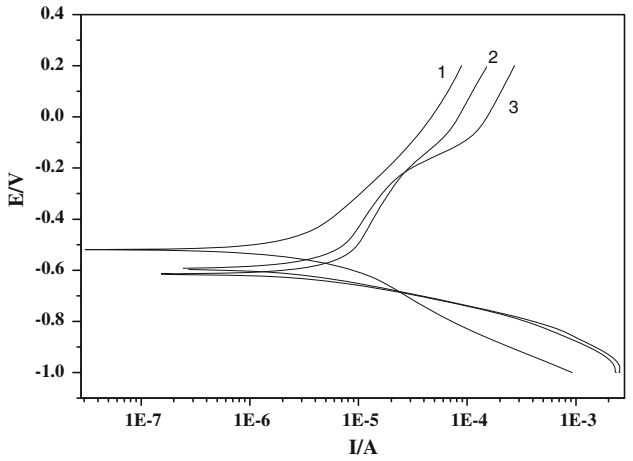

Fig. 4 E-log *I* polarization curves for bare aluminum in 0.1 M H_2SO_4 solution

created by the electrochemical process, its value reflects all of the processes causing corrosion (how fast corrosion will occur) and the ''corrosion current'' reflects the magnitude of corrosion or rate of corrosion.

Figure 4 shows the polarization curves of uncoated aluminum recorded in three subsequent scans in 0.5 M H_2SO_4 solution at the scan rate of 5 mVs^{-1}. Table 3 shows the results of corrosion data interpreted from Tafel slope. Aluminum, in general is corrosion resistant because of the protective alumina film formed on its surface; this film is quite stable in aqueous solutions where the pH is between 4.0 and 8.5. The oxide film is naturally self-renewing and accidental abrasion or other mechanical damage of the surface film is rapidly repaired (Ref 24, 25). In the 1st scan (Fig. 4), the corrosion potential was −520 mV indicating active corrosion of the metal. This happens because the real surface comprises various types of defects. The total area occupied by such defects is low, (in 99.99% Al it is only 0.2% of the surface); however, it still bears a large impact on the corrosion performance and durability of the aluminum. The defects filled with the acid provide anodes,

Table 3 Corrosion currents and corrosion potentials calculated from E-log *I* polarization curves for all the gold-plated samples

Sample	No. of scan	E_{corr}, V	I_{corr}, A
Uncoated Al	1	−0.520	2.9×10^{-6}
	2	−0.615	6.2×10^{-6}
	3	−0.595	4.8×10^{-6}
Au-w-o-1	1	−0.190	1.4×10^{-5}
	2	−0.183	1.0×10^{-5}
	3	−0.186	1.0×10^{-5}
Au-w-u-1	1	+0.043	5.2×10^{-6}
	2	−0.003	9.2×10^{-6}
	3	−0.065	5.8×10^{-6}
Au-w-o-2	1	−0.003	7.8×10^{-6}
	2	−0.060	1.2×10^{-6}
	3	−0.133	1.1×10^{-6}
Au-w-u-2	1	+0.103	3.5×10^{-6}
	2	+0.043	7.5×10^{-6}
	3	+0.029	7.1×10^{-6}

while the residual metallic impurities act as cathodes. At all temperatures, the electrochemical reaction,

$$Al \rightarrow Al^{3+} + 3e \quad E_0 = -1.66V \qquad \text{(Eq 1)}$$

is more electronegative than the hydrogen evolution reaction so that the anodic reaction is the limiting reaction. The second scan shows a different history. The corrosion potential becomes more negative, i.e., −615 mV while the corrosion current decreased (6.2×10^{-6} A) implying enhanced corrosion of aluminum but with lower rate of dissolution. It appears paradoxical but in reality it is not so. Once the Al^{3+} ions are formed, they tend to react with water molecules to form aluminum hydroxide as,

$$Al^{3+} + 3H_2O \rightarrow Al(OH)_3 + 3H^+ \quad E_0 = -1.55V \qquad \text{(Eq 2)}$$

The product forms a passive film on the surface and hinders further dissolution of metal so that electrons needed for the reduction of protons is not available. This explains the decrease

in corrosion current. The alkaline local pH tends to shift the corrosion potential to more negative direction (Ref 26). It is known that a passive surface is more corrosion-resistant than an active surface. The result of third scan is not so different from the second scan except for a minor variation.

The purpose of gold plating is to prevent corrosion as it is the most nonreactive of all metals and is benign in all natural and industrial environments. Gold never reacts with oxygen (one of the most active elements), which means it will not rust or tarnish. Gold is among the most electrically conductive of all metals. Gold is able to convey even a tiny electrical current in temperatures varying from −55 to +200 °C. "Purple plague" is a brittle gold aluminum compound formed when bonding gold to aluminum. The growth of such a compound can cause failure in microelectronic interconnection bonds. In order to avoid this complication, nickel strike is preferred as an intermediate step.

Figure 5 shows the E-log *I* polarization curves for the (single zincated, unsonicated) Au-w-o1 sample. Corrosion (or mixed) potential was −190 mV in the initial scan; this value did not change noticeably in the subsequent scans. As expected, the shift in corrosion potential was in the positive direction by 330 mV as against bare aluminum, an indicative of corrosion-resistant surface. Surprisingly, corrosion current was higher than the uncoated aluminum; it shows an increase in the rate of corrosion; this means that the corrosion occurs at a higher rate at lower equilibrium potential.

Such an interpretation would hold well for any active metal surface but not for a noble metal-like gold which do not undergo corrosion in acids and alkali solutions. It is known that corrosion potential is also a mixed potential involving both anodic and cathodic reactions and gold is a very good catalyst in fuel cell reactions (Ref 27). In fact it is used along with platinum to enhance the hydrogen evolution reaction. So the mixed potential of −190 mV was due the following reactions on the gold surface:

$$\text{Cathodic reaction: } 2H^+ + 2e \rightarrow H_2 \uparrow \quad E_0 = 0V \qquad \text{(Eq 3)}$$

$$\text{Anodic reaction: } H_2O \rightarrow 1/2O_2 + 2H^+ + 2e \quad E_0 = 1.229V \qquad \text{(Eq 4)}$$

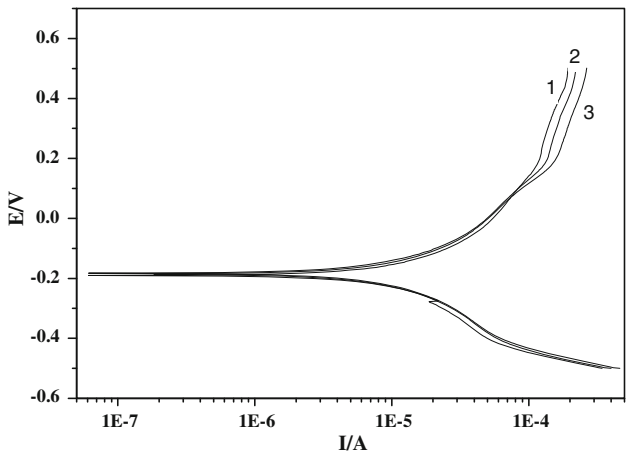

Fig. 5 E-log *I* polarization curves for Au-w-o-1 (gold-plated sample with single zincating and without sonication)

Increase in corrosion current as against the bare aluminum surface is a pointer to catalytic behavior of gold to hydrogen in acid solution.

In Au-w-u-1 sample, mixed potential was shifted to the noble direction by 157 mV (as compared to Au-w-o-1) in the initial scan; the value was 43 mV (Fig. 6; Table 3). Such a response is a measure of stability of the gold-plated surface to corrosive environment. In the second and third scans, the potentials were 0.0 and −65 mV, respectively. Such a change in mixed potential denotes a change in metallic surface, most probably could be due to the corrosion of layer beneath the fold layer. This could occur if the thickness of gold plating is very low or there exists defect in the gold-plated surface. This reaction could favor the cathodic reaction which would shift the mixed potential toward active direction. Initial shift of mixed potential recorded in the very first scan is a signature of surface morphology determined by the plating parameters.

For Au-w-o-2 sample, E-log *I* polarization curves recorded are shown in Fig. 7; in this case, the pretreatment includes double zincation but without ultrasonication. On comparing the single zincated (Au-w-o-1) and double zincated (Au-w-o-2)

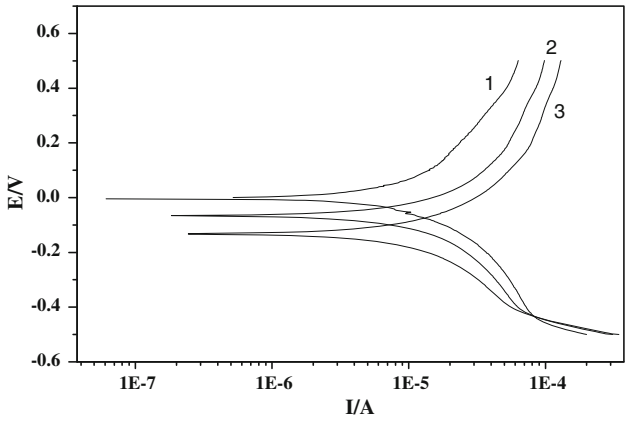

Fig. 6 E-log *I* polarization curves for Au-w-o-2 (gold-plated sample with double zincating and without sonication)

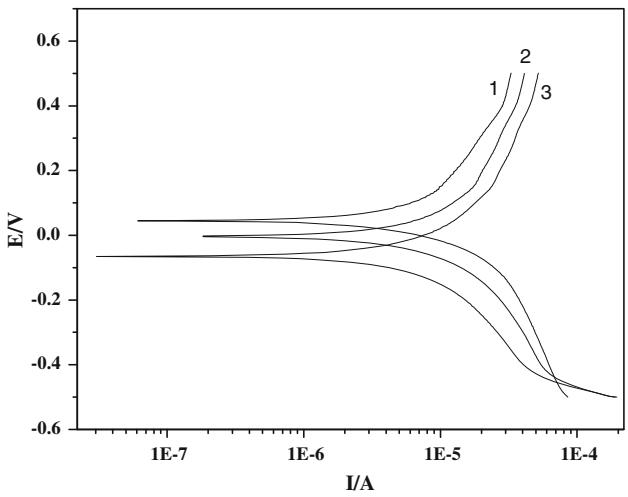

Fig. 7 E-log *I* polarization curves for Au-w-u-1 (gold-plated sample with single zincating and with sonication)

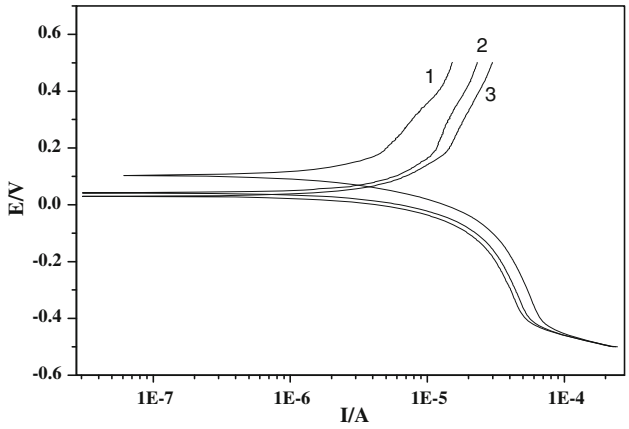

Fig. 8 E-log *I* polarization curves for Au-w-u-2 (gold-plated sample with double zincating and with sonication)

(without ultrasonication) samples, it was clear that Au-w-o-2 sample gives a positive shift to the mixed potential. The shift was 187 mV in the positive direction. Therefore, double zincation is more preferable and beneficial during the pretreatment step so that better gold plating can be attained. Subsequent scans show a shift of potential toward negative direction whose behavioral pattern is similar to that of Au-w-u-1 sample.

Figure 8 shows the E-log *I* polarization curve for the Au-w-u-2 sample. This sample shows the best result; the initial scan revealed the mixed potential at 103 mV. This sample underwent double zincation as well as ultrasonication. A 100 mV shift toward noble direction against Au-w-o-2 sample was noted. This favorable result could be attributed to solely the sonication during the zincation step. The benefit of double zincation against single zincation aided by ultrasonication may be understood by the mixed potentials of Au-w-u-1 and Au-w-u-2 samples; they were 43 and 103 mV, respectively. The shift was 60 mV. So, both sonication and double zincation play a crucial role in determining the surface morphology, uniformity, and particle growth of gold during the plating which in turn decides the immunity of the surface to the corrosive environment.

3.3 Pull-Off Adhesion Test

The adhesion strength of the gold coatings on Al/Ni substrates was measured with a pull off tester. In the pull test, the specimens for each test were glued onto an aluminum stud (dolly) of 20 mm diameter with epoxy, followed by curing at room temperature for 24 h. The dollies were subject to pulling using a manual hydraulic system. Table 4 shows the results obtained for all the samples and Fig. 9 shows the dolly and specimen after the completion of the test. The figure reveals the precise failure of the coated layer along the edge of the dolly. For a poorly adherent surface, the edges would break and film would be peeled off from surface beyond the dolly edge. Ultrasonicated, double zincated sample gave the highest adhesion while the double zincated sample without sonication gave the lowest value. The critical load values measured from the pull test showed that the ultrasonic agitation during zincating treatment enhanced the adhesion of the Au coatings on Al/Ni substrates.

Table 4 Pull off adhesion test results

S. No.	Coating	Load required for pull-off, MPa
1	Au-w-o-1	0.73
2	Au-w-o-2	0.63
3	Au-w-u-1	0.97
4	Au-w-u-2	1.78

Fig. 9 Test sample and dolly after pull-off adhesion test

4. Conclusions

We showed that the significant adhesion strength enhancement of gold-plated layers on Al/Ni substrates can be attained by applying ultrasonic agitation during zincating. Ultrasonic agitation during zincating produced the dense population of small Zn particles and increased the coverage of a Zn intermediate layer. The uniform Zn layer and the sufficient coverage of Zn particles on Al surface increased the adhesion between Ni and Al surface as well as the Ni and Au surface. Gold-plated sample prepared under ultrasonication and double zincation gave the best results in the adhesion pull off test which is good measure of adhesion strength of gold coating to the substrate. SEM images of the same sample show spindle-like gold particles dispersed uniformly with a fine coverage of substrate. E-log *I* polarization studies confirmed the higher corrosion resistance of this sample under the present experimental conditions as indicated by the positive corrosion potentials. Hence, we claim that double zincation during ultrasonic agitation produces the best substrate for electrochemical plating of nickel and gold.

Acknowledgment

The authors would like to thank their colleagues Mr. P. K. P. Rupa and Dr. R. M. Mohanty for helping to conduct the pull-off adhesion test.

References

1. D.A. Doane and P.D. Franzon, Ed., *Multichip Module Technologies and Alternatives: The Basics*, Van Nostrand Reinhold, New York, 1980
2. E. Zakel and H. Reichl, *Flip Chip Technologies*, J.H. Lau, Ed., McGraw-Hill, New York, 1996,
3. K. Wong, K. Chi, and A. Rangappan, Application of Electroless Nickel Plating in the Semiconductor Microcircuit Industry, *Plat. Surf. Finish.*, 1988, **75**(7), p 70–77
4. J. Simon, E. Zakel, and H. Reichl, Electroless. Deposition of Bumps for TAB Technology, *Met. Finish.*, 1990, **88**(10), p 23–26
5. A. Aintila, E. Jarvinen, and S. Lalu, *Proceedings of IEMT*, Kanazawa, Japan, 1993, p 33
6. F.C. Tai, K.J. Wang, and J.G. Duh, Application of Electroless Ni–Zn–P Film for Under-Bump Metallization on Solder Joint, *Scripta Mater.*, 2009, **61**(7), p 748–751
7. M.O. Alam, Y.C. Chan, and K.C. Hung, Reliability Study of the Electroless Ni–P Layer Against Solder Alloy, *Microelectron. Reliab.*, 2002, **42**(7), p 1065–1073
8. A. Aintila, A. Bjorklof, E. Jarvinen, and S. Lalu, *Proceeding of the IEEE/CPMT, International Electronics Manufacturing Technology Symposium*, 1994, p 160
9. A. Bjorklof, Electroless Bumped Bare Dice on Flexible Substrates, *Microelectron Int.*, 1996, **13**(2), p 49–52
10. T. Ohtsuka, T. Kawakita, H. Fujimoto, and K. Hatada, *Proceeding of the Joint International Electronic Manufacturing Symposium and International Microelectronics Conference*, 1997, p 169
11. J. Kloeser, A. Ostmann, J. Gwiasda, F. Bechtold, R. Aschenbrenner, and H. Reichl, Low Cost Flip Chip Technologies on Chemical Nickel Bumping and Solder Printing, *Int. J. Microcircuits Electron. Packag.*, 1997, **20**, p 383–389
12. G. Qi, X. Chen, and Z. Shao, Influence of Bath Chemistry on Zincate Morphology on Aluminum Bond Pad, *Thin Solid Films*, 2002, **406**(1–2), p 204–209
13. K. Azumi, T. Yugiri, M. Seo, and S. Fujimoto, Double Zincate Pretreatment of Sputter-Deposited Al Films, *J. Electrochem. Soc.*, 2001, **148**(6), p 433–439
14. K.-L. Lin and S.-Y. Chang, The Morphologies and the Chemical States of the Multiple Zincating Deposits on Al Pads of Si Chips, *Thin Solid Films*, 1996, **288**(1–2), p 36–40
15. G. Qi, L.G.J. Fokkink, and K.H. Chewb, Zincating Morphology of Aluminum Bond Pad: Its Influence on Quality of Electroless Nickel Bumping, *Thin Solid Films*, 2002, **406**(1–2), p 219–223
16. T.J. Mason, *Sonochemistry, The Uses of Ultrasonic in Chemistry*, Royal Society of Chemistry, Cambridge, 1990
17. R. Walker, Ultrasound Improves Electrolytic Recovery of Metals, *Ultrason. Sonochem.*, 1997, **4**, p 39–43
18. J.-Gi. Jin, S.-Ki. Lee, and Y.-Ho. Kim, Adhesion Improvement of Electroless Plated Ni Layer by Ultrasonic Agitation During Zincating Process, *Thin Solid Films*, 2004, **466**, p 272–278
19. A. Koshio, M. Yudasaka, M. Zhang, and S. Iijima, Simple Way to Chemically React Single-Wall Crabon Nanotubes with Organic Materials Using Ultrasonication, *Nano Lett.*, 2001, **1**(7), p 61–73
20. P.X. Hou, S. Bai, Q.H. Yang, C. Liu, and H.M. Cheng, Multi-Step Purification of Carbon Nanotubes, *Carbon*, 2002, **40**(1), p 81–85
21. M.A. Saad, *Compressible Fluid Flow*, Prentice Hall, Englewood Cliffs, NJ, 1993
22. S.S. Michael, C.M. Valerie, K.M. Michael, J.A. Mathew, H.H. Erik, and K. Carter, The Role of Surfactant Adsorption during Ultrasonication in the Dispersion of Single-Walled Carbon Nanotubes, *J. Nanosci. Nanotechnol.*, 2003, **3**(1–2), p 81–86
23. P. He, Y. Gao, J. Lian, L. Wang, D. Qian, J. Zhao, W. Wang, M.J. Schulz, X.P. Zhou, and D. Shi, Surface Modification and Ultrasonication Effect on the Mechanical Properties of Carbon Nanofiber/Polycarbonate Composites, *Composites A*, 2006, **37**, p 1270–1275
24. M. Pourbaix, *Atlas of Electrochemical Equilibria in Aqueous Solutions*, NACE Cebelcor, Huston, 1974
25. J.R. Davis, Ed., *Metals Handbook*, Vol 13, 9th ed., ASM International, Materials Park, OH, 1987
26. M. Jayalakshmi, W.-Y. Kim, K.-D. Jung, and O.-S. Joo, Electrochemical Characterization of Ni-Mo-Fe Composite Film in Alkali Solution, *Int. J. Electrochem. Sci.*, 2008, **3**(8), p 908–917
27. D. Cameron, R. Holliday, and D. Thompson, Gold's Future Role in Fuel Cell Systems, *J. Power Sour.*, 2003, **118**(1–2), p 298–303